Human Molecular Genetics, 2013, Vol. 22, No. 19 **3869–3882**
doi:10.1093/hmg/ddt242
Advance Access published on May 29, 2013

A role of mitochondrial complex II defects in genetic models of Huntington's disease expressing N-terminal fragments of mutant huntingtin

Maria Damiano[1,2,3,†], Elsa Diguet[1,2,3,†], Carole Malgorn[1,2], Marilena D'Aurelio[3], Laurie Galvan[1,2], Fanny Petit[1,2], Lucile Benhaim[1,2], Martine Guillermier[1,2], Diane Houitte[1,2], Noelle Dufour[1,2], Philippe Hantraye[1,2], Josep M. Canals[4], Jordi Alberch[4], Thierry Delzescaux[1,2], Nicole Déglon[1,2,‡], M. Flint Beal[3] and Emmanuel Brouillet[1,2,*]

[1]CEA, DSV, I[2]BM, Molecular Imaging Research Center (MIRCen), Fontenay-aux-Roses F-92265, France, [2]CNRS, CEA URA 2210, Fontenay-aux-Roses F-92265, France, [3]Department of Neurology and Neuroscience, Weill Cornell Medical College, Cornell University, New York, NY, USA and [4]Department of Cell Biology, Immunology and Neuroscience, Medical School, IDIBAPS, CIBERNED, University of Barcelona, Barcelona, Spain

Received February 12, 2013; Revised and Accepted May 23, 2013

Huntington's disease (HD) is a neurodegenerative disorder caused by an abnormal expansion of a CAG repeat encoding a polyglutamine tract in the huntingtin (Htt) protein. The mutation leads to neuronal death through mechanisms which are still unknown. One hypothesis is that mitochondrial defects may play a key role. In support of this, the activity of mitochondrial complex II (C-II) is preferentially reduced in the striatum of HD patients. Here, we studied C-II expression in different genetic models of HD expressing N-terminal fragments of mutant Htt (mHtt). Western blot analysis showed that the expression of the 30 kDa Iron–Sulfur (Ip) subunit of C-II was significantly reduced in the striatum of the R6/1 transgenic mice, while the levels of the FAD containing catalytic 70 kDa subunit (Fp) were not significantly changed. Blue native gel analysis showed that the assembly of C-II in mitochondria was altered early in N171-82Q transgenic mice. Early loco-regional reduction in C-II activity and Ip protein expression was also demonstrated in a rat model of HD using intrastriatal injection of lentiviral vectors encoding mHtt. Infection of the rat striatum with a lentiviral vector coding the C-II Ip or Fp subunits induced a significant overexpression of these proteins that led to significant neuroprotection of striatal neurons against mHtt neurotoxicity. These results obtained *in vivo* support the hypothesis that structural and functional alterations of C-II induced by mHtt may play a critical role in the degeneration of striatal neurons in HD and that mitochondrial-targeted therapies may be useful in its treatment.

INTRODUCTION

For reasons that are still unclear, the striatum is preferentially damaged in a number of acute and chronic pathological conditions, leading to devastating cognitive deficits and abnormal movements (1). The most studied of these illnesses is Huntington's disease (HD).

HD is a dominantly inherited disorder generally affecting young adults. Symptoms include involuntary abnormal movements (chorea, dyskinesia, dystonia), frontal cognitive deficits (e.g. alterations of adaptation) and psychiatric disturbances (2). The disease is fatal ~15 years after the onset of symptoms. There is no treatment available to slow the progression of this devastating disorder.

*To whom correspondence should be addressed at: Neurodegenerative Disease Laboratory, URA CEA-CNRS 2210, Molecular Imaging Research Center, CEA, 18 route du Panorama, BP6, 92265 Fontenay-aux-Roses, France. Tel: +33 146549622; Fax: +33 146549116; Email: emmanuel.brouillet@cea.fr
†The first two authors contributed equally to the present study.
‡Present address: Lausanne University Hospital, Laboratory of Cellular and Molecular Neurotherapies, CH-1011 Lausanne, Switzerland.

© *The Author 2013. Published by Oxford University Press.*
This is an Open Access article distributed under the terms of the Creative Commons Attribution Non-Commercial License (http://creativecommons.org/licenses/by-nc/3.0/), which permits non-commercial re-use, distribution, and reproduction in any medium, provided the original work is properly cited. For commercial re-use, please contact journals.permissions@oup.com

HD is caused by a mutation in the gene encoding the protein huntingtin (Htt) that consists in a CAG triplet repeat expansion translated into an abnormal polyglutamine (polyQ) tract within the N-terminal region of the protein (3). While mutant Htt (mHtt) protein is ubiquitously expressed in the brain, degeneration primarily affects the striatum (4).

Mechanisms of HD pathogenesis are likely multifactorial. The polyQ expansion in mHtt produces a gain of function that is toxic to neurons through several mechanisms. One major early event in HD is the alteration of transcription (5). Other early alterations includes intracellular signaling defects, axonal transport alterations, deregulated autophagy, alteration of synaptic function, defects in brain derived neurotrophic factor transcription, secretion and transport (3), perturbation of calcium homeostasis (6) and mitochondrial defects (7,8).

Compelling evidence supports a role of energy defects (9) and more specifically mitochondrial dysfunctions in HD pathogenesis (1,10). mHtt interacts with mitochondria, and a reduction in mitochondrial membrane potential is present in various genetic models of HD, as well as in lymphoblasts isolated from HD patients (11,12). mHtt interacts with the protein DRP1 altering transport and fusion of mitochondria (13). The biogenesis of mitochondria in HD may also be altered, especially through mechanisms involving down-regulation of PGC-1α (14). How these anomalies progressively change the efficiency of the respiratory chain and oxidative phosphorylation is unknown. However, anomalies in the enzymes of the respiratory chain have been also reported in the striatum of HD patients. In particular, the activity of mitochondrial complex II (C-II) has been consistently found to be reduced in the striatum of HD patients (15,16). The loss of C-II activity in the striatum of HD patients is associated with a reduced expression of two subunits of C-II, the Iron–sulfur subunit (Ip, 30 kDa) and FAD subunit (Fp, 70 kDa) (17). We demonstrated a similar loss of C-II subunits and activity in striatal neurons in primary culture, following transduction with lentiviral vectors encoding the N-terminal fragment of mHtt carrying the expanded polyQ tract (17,18). Of interest, the overexpression of C-II Ip or Fp subunits has been found to be neuroprotective against mHtt toxicity in this *in vitro* model, suggesting a key role of C-II in HD pathogenesis. However, the potential mechanisms underlying the reduction in Ip expression in HD remain unknown. The defects in C-II have been rarely assessed *in vivo* in HD animal models and results are not congruent. No obvious reduction in C-II levels was observed in a knock-in mouse model of HD (19). A comprehensive review on mitochondria in HD suggested no loss of C-II activity in transgenic mouse models of HD (10). However, longitudinal proteomic analysis of R6/2 mice recently indicated that the expression of the Ip subunit significantly varies during the course of the disease, with early increases in expression (20). Thus, the potential role of C-II defects in HD remains unclear.

Here, we aimed at elucidating whether the expression of mHtt may lead to a defect in C-II *in vivo*. To address this question, we examined C-II activity and expression of subunits constituents in two mouse models of HD (N171-82Q and R6/1) (21,22) and in a rat model of HD using lentiviral vectors coding the N-terminal 171 amino acids of mHtt with 82 glutamines (lenti-171-82Q). We observed a preferential loss of C-II expression and activity in these HD models *in vivo*. We then examined whether the overexpression of C-II subunits using lentiviral vectors exerts neuroprotection against mHtt toxicity in the rat striatum.

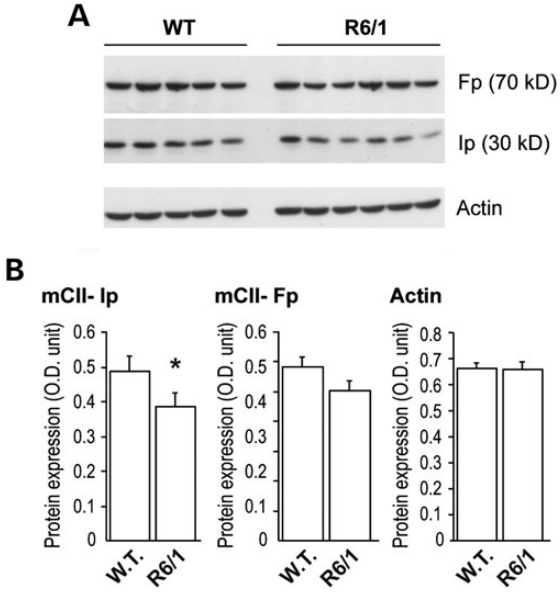

Figure 1. Change in C-II subunits in R6/1 mice. The striatum was dissected out from 16-week-old mice transgenic for human mHtt exon 1 and analyzed by western blot. Equal amount of proteins was loaded in each lane. Each lane represents a different mouse. (**A**) Typical western blot of samples showing the expression of Fp, Ip and actin in striatal samples. (**B**) Histograms corresponding to the quantification of the expression of the proteins by image analysis. Note that there is a significant loss of SDH subunit Ip, while only a trend is seen for the Fp subunit. Results are the mean ± SEM. $^{*}P < 0.02$, unpaired Student's *t*-test.

RESULTS

Early decrease in the levels of assembled complex II in brain mitochondria in transgenic mice expressing an N-terminal fragment of mHtt

The pathogenic role of the changes in C-II expression or activity is debated and has not been systematically assessed in different genetic models of HD (see Introduction). For this reason, we analyzed C-II expression in the striatum of three different models expressing the N-terminal fragment of mHtt.

We first studied the levels of C-II subunits Ip and Fp in the striatum of the R6/1 transgenic mouse model of HD. To do this, western blot analysis was carried out on total protein homogenates. Results showed that the Ip expression levels were significantly decreased in the striatum of R6/1 mice when compared with wild-type littermates at 16 weeks of age (mean ± SEM: wild-type, $n = 5$, 0.516 ± 0.041 OD unit; R6/1, $n = 6$, 0.387 ± 0.040 OD unit; unpaired Student's *t*-test, $P < 0.05$; Fig. 1). A mild reduction in Fp levels in R6/1 was not statistically significant (wild-type, $n = 5$, 0.596 ± 0.078 OD unit; R6/1, $n = 6$, 0.503 ± 0.082 OD unit; unpaired Student's *t*-test, $P > 0.089$). Levels of actin was similar in all groups (wild-type, $n = 5$, 0.68 ± 0.016 OD unit; R6/1, $n = 6$, 0.66 ± 0.029 OD unit; unpaired Student's *t*-test, $P < 0.05$). Normalization of Ip and Fp protein to actin levels confirmed selective loss of Ip subunit (Ip/actin ratio: wild-type, $n = 5$, 0.762 ± 0.061; R6/1, $n = 6$,

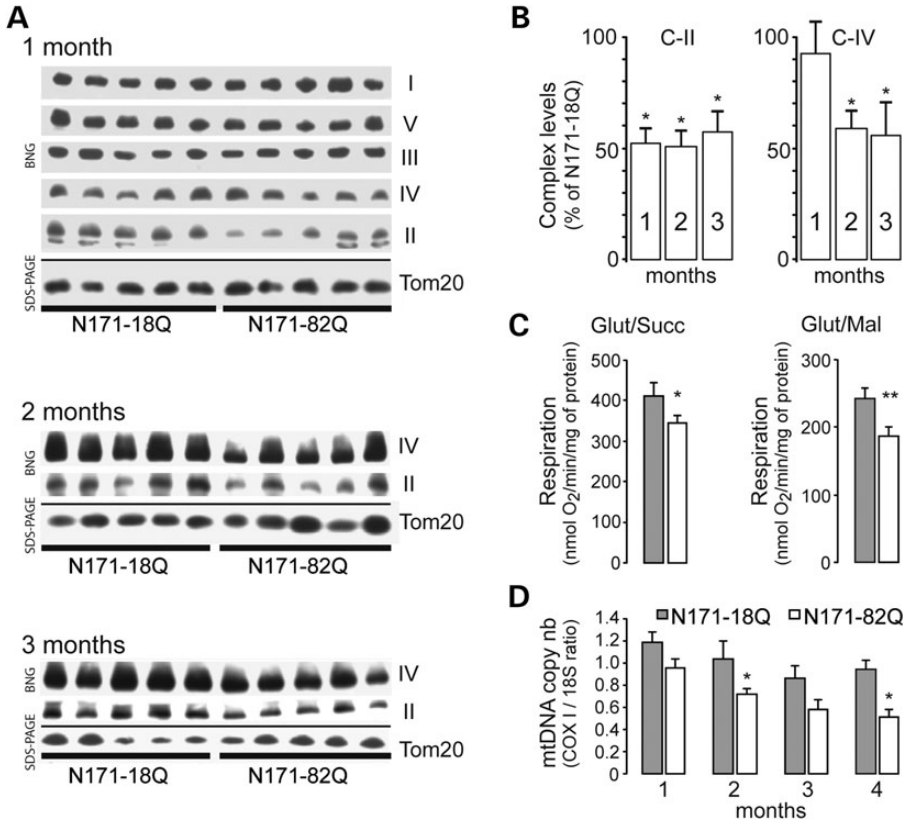

Figure 2. Mitochondrial defects in mitochondria isolated from N171-82Q transgenic mice. Mitochondria were isolated from the forebrain of N171-82Q transgenic mice and controls (N171-18Q mice) and analyzed by blue native gel (BNG) electrophoresis to detect assembled mitochondrial complexes (**A** and **B**) and evaluate respiration (**C**) and mtDNA copy number (**D**). In (A) are shown representative BN-PAGE from samples prepared with mice at different ages. Levels of Tom20 as detected using western blot were used to control for the quantity of mitochondria in each lane. Note that at 1 month, C-II levels are lower in HD transgenic mice when compared with controls, while other complexes remained essentially unchanged. (B) Quantification of complexes levels is shown. At later time points, C-IV levels are also reduced. Results are the mean ± SEM. $^{*}P < 0.05$. (C) Respiration of mitochondria preparation was determined using either glutamate/succinate 5:2 mM (complex II) or substrates glutamate/malate 5:1 mM (complex I) at 2 and 3 months of age, respectively. Results are the mean ± SEM. $^{*}P < 0.05$; $^{**}P < 0.02$. (D) Evaluation of the mtDNA copy number assessed by the ratio between COX1 mRNA and 18S mRNA levels measured by RT-PCR. Results are the mean ± SEM. $^{*}P < 0.05$.

0.584 ± 0.044; unpaired Student's *t*-test, $P < 0.037$; Fp/actin ratio: wild-type, $n = 5$, 0.881 ± 0.055; R6/1, $n = 6$, 0.768 ± 0.051; unpaired Student's *t*-test, n.s.; $P > 0.168$).

We next examined whether the assembly of C-II could be modified when compared with the other respiratory chain complexes. For this, mitochondria were prepared using the forebrain of N171-82Q and control mice and analyzed using blue native polyacrylamide gel electrophoresis (BN-PAGE). We found that the amount of assembled C-II was significantly decreased in brain mitochondria isolated from 1-month-old N171-82Q mice, when compared with those from N171-18Q mice (Fig. 2A; mean ± SEM: N171-82Q, $n = 5$, 51.39 ± 7.18% of N171-18Q levels; unpaired Student's *t*-test, $P < 0.001$). At this early time point, the levels of the other complexes were similar in N171-82Q when compared with controls (Fig. 2). The comparison between N171-82Q and both N171-18Q littermates revealed that the defective assembly of C-II persisted at later stages of the disease, at 2 months of age (N171-82Q, $n = 5$, 50.78 ± 8.85 of N171-18Q levels; unpaired Student's *t*-test, $P < 0.001$) and at 3 months of age (N171-82Q, $n = 5$, 59.43 ± 6.8% of N171-18Q levels; unpaired Student's *t*-test, $P < 0.001$). The differences between N181-82Q and non-transgenic littermates became also significant at these time points (2 months: N171-82Q, $n = 5$, mean ± SEM: 41.6% ± 4.1% of non-transgenic littermates levels; unpaired Student's *t*-test, $P < 0.001$, not shown; 3 months: N171-82Q, $n = 4$, mean ± SEM: 29.1 ± 7.6% of non-transgenic littermates levels; unpaired Student's *t*-test, $P = 0.0001$, not shown). C-IV assembly was also significantly defective at these later time points when N171-82Q mice were compared with N171-18Q mice (Fig. 2; N171-82Q at 2 months, $n = 5$, 58.4 ± 6.7% of N171-18Q levels, $P < 0.001$; N171-82Q at 3 months, $n = 5$, 54.9 ± 9.9% of N171-18Q levels, unpaired Student's *t*-test, $P = 0.001$). At 3 months, C-IV levels were also found to be reduced when N171-82Q mice were compared with those determined in non-transgenic mice (N171-82Q, $n = 4$, 31.8 ± 5.4% of non-transgenic littermates levels, unpaired Student's *t*-test, $P < 0.001$, not shown). Transient time point changes seen in the amount of assembled C-V and C-III were seen in the comparison between brain mitochondria isolated from N171-82Q mice and non-transgenic littermates at 1 (C-V) and 2 months (C-V and C-III) or in the comparison between brain mitochondria isolated from N171-18Q mice and non-transgenic littermates (C-V) at 1 month of age (not shown). Although defects in the functions of these two complexes have

been reported to be relevant in the pathogenesis of HD (23,24), by comparing the transgenic N171-18Q with age-matched N171-82Q, these differences were no longer visible.

Oxygen consumption was also measured on freshly isolated mitochondria of N171-82Q and control mice. Results revealed that brain mitochondria from N171-82Q mice at 2 months of age had a significant defect in the state 3 respiration using glutamate/succinate as C-II substrates (non-transgenic, $n = 6$, 412.8 ± 27.2 O_2/min/mg of protein; N171-82Q, $n = 6$, 344.3 ± 12.1 nmol O_2/min/mg of protein; unpaired Student's t-test, $P < 0.05$; Fig. 2C). No alteration was seen in the presence of glutamate/malate as C-I substrates (not shown). At 3 months of age, mitochondria from N171-82Q showed reduced state 3 respiration using C-I substrates, when compared with N171-18Q mitochondria (Fig. 2C; N171-18Q, $n = 6$, 240.9 ± 13.5 O_2/min/mg of protein; N171-82Q, $n = 6$, 188.1 ± 12.0 nmol O_2/min/mg of protein; unpaired Student's t-test, $P < 0.02$). Thus, early functional alterations of C-II occur in 171-82Q mice.

To determine whether any other nuclear-driven mitochondrial functions other than C-II assembly were defective in transgenic mHtt models of HD, we quantified the mtDNA copy number using cytochrome *c* oxidoreductase (COX)1 versus the nuclear 18S gene amplification rate using quantitative real-time quantitative reverse transcriptase-polymerase chain reaction (qRT-PCR). This assay requires only a little amount of tissue, and it was therefore possible to perform it on total DNA isolated selectively from striata of N171-82Q and N171-18Q mice, at different stages (Fig. 1D). A progressive decline in the amount of mtDNA was found in the striatum of N171-82Q mice when compared with N171-18Q. This difference was observed in the animals at pre-symptomatic ages (1 month) and became bigger thereafter. Statistical analysis showed that the reduction was linked to genotype and aggravated with age ($n = 5–11$; two-way ANOVA; gene, $F = 52.98$, $P < 0.005$; age, $F = 14.71$, $P < 0.027$) and differences were significant at 2 and 4 months of age ($P < 0.05$ and $P < 0.004$, respectively, using pairwise multiple comparison procedure with the Holm–Sidak method). This observation indicated reduced mitochondrial biogenesis in N171-82Q mice.

Reduced striatal levels of complex II in a rat model expressing a short N-terminal fragment of mHtt

We studied whether the expression of mHtt could produce changes in C-II expression or activity in a rat model of HD (25). In this rat model, intrastriatal injection of lentiviral vectors coding mHtt are used, leading to a first phase of mild neuronal dysfunction (2–8 weeks) followed by a phase of actual degeneration (10–12 weeks) (26–28). The severity of the lesions produced by lentiviral vectors encoding mHtt can be assessed using biochemical markers of neuronal integrity such as DARPP-32 (dopamine- and cAMP-regulated phosphoprotein, 32 kDa), COX and NeuN (neuronal nuclei marker, i.e. Fox-3). The series of experiments performed in the rat model is presented in Figure 3.

We assessed the effect of mHtt on C-II activity using *in situ* succinate dehydrogenase (SDH) histochemistry and image

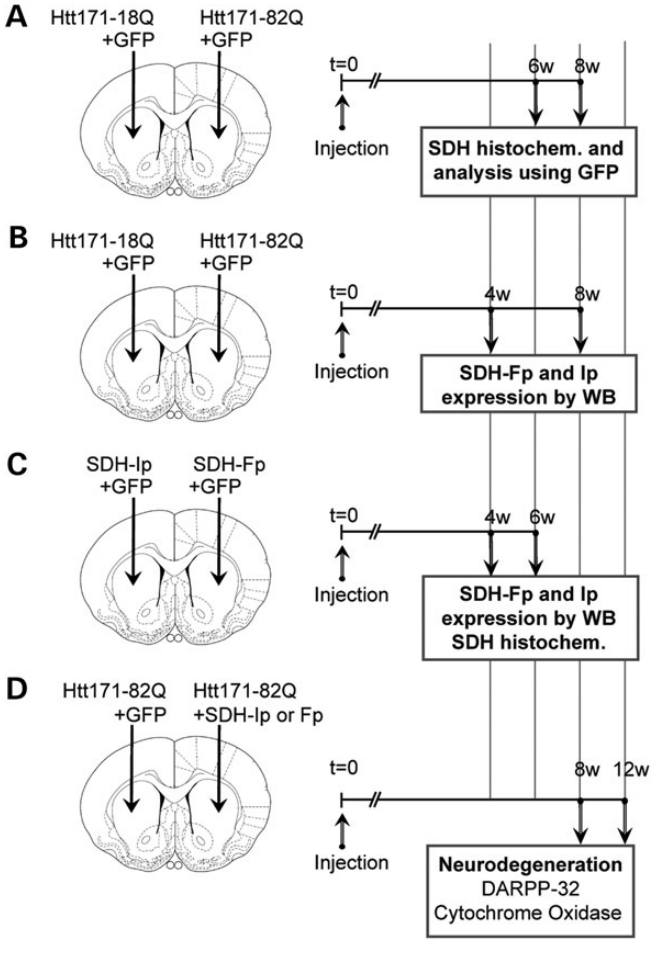

Figure 3. Experimental design to study mitochondrial complex II expression change induced by mHtt in rats. In all experiments, adult rats received a stereotaxic injection of lentiviral vectors (4 μl). Animals were infected with a lentiviral vector encoding the 171 N-terminal amino acids of mHtt with 82 polyQ repeats (Htt171-82Q), or the corresponding wild-type fragment with 18 polyQ repeats (Htt171-18Q) with the reporter fluorescent protein green fluorescent protein (GFP) or vectors coding the C-II Fp or Ip subunit. In the first experiment (**A**), rats were injected with lentiviral vectors (4 μl) encoding GFP (left and right striatum, 100 ng/μl of p24) plus either Htt-171-82Q (right striatum, 150 ng/μl of p24) or Htt-171-18Q (left striatum, 150 ng/μl of p24). Semi-quantitative evaluation of C-II activity using histochemistry of SDH activity was performed at 6 weeks to analyze the co-localization of SDH activity with GFP and the 3D measurement of SDH activity in the area showing SDH depletion. In the second experiment (**B**), rats were injected with lentiviral vectors (4 μl) encoding GFP (left and right striatum, 100 ng/μl of p24) plus either Htt-171-82Q (right striatum, 150 ng/μl of p24) or Htt-171-18Q (left striatum, 150 ng/μl of p24). Rats were killed at 6 weeks post-surgery. Striatal punches of the fluorescent area were made to prepared tissue homogenate to perform western blot analysis of Fp, Ip and actin expression. In the third experiment (**C**), rats were injected with lentiviral vectors (4 μl) encoding GFP (left and right striatum, 100 ng/μl of p24) plus either lenti-Fp (right striatum, 150 ng/μl of p24) or lenti-Ip (left striatum, 150 ng/μl of p24). Rats were killed at 4 weeks post-surgery. Striatal punches were made to prepared tissue homogenate to perform western blot analysis of C-II subunits Fp and Ip and Tom20. In addition, rats were also injected to perform SDH histochemistry. In the fourth experiment (**D**), rats were co-injected with lentiviral vectors (4 μl) encoding wt-Htt171-18Q fragment or mHtt171-82Q fragment (100 ng/μl of p24) plus either Fp (150 ng/μl of p24), Ip (150 ng/μl of p24) or GFP as a control of viral load. Rats were killed at 12 weeks post-surgery and processed for the evaluation of striatal degeneration using DARPP-32 immunohistochemistry and COX histochemistry.

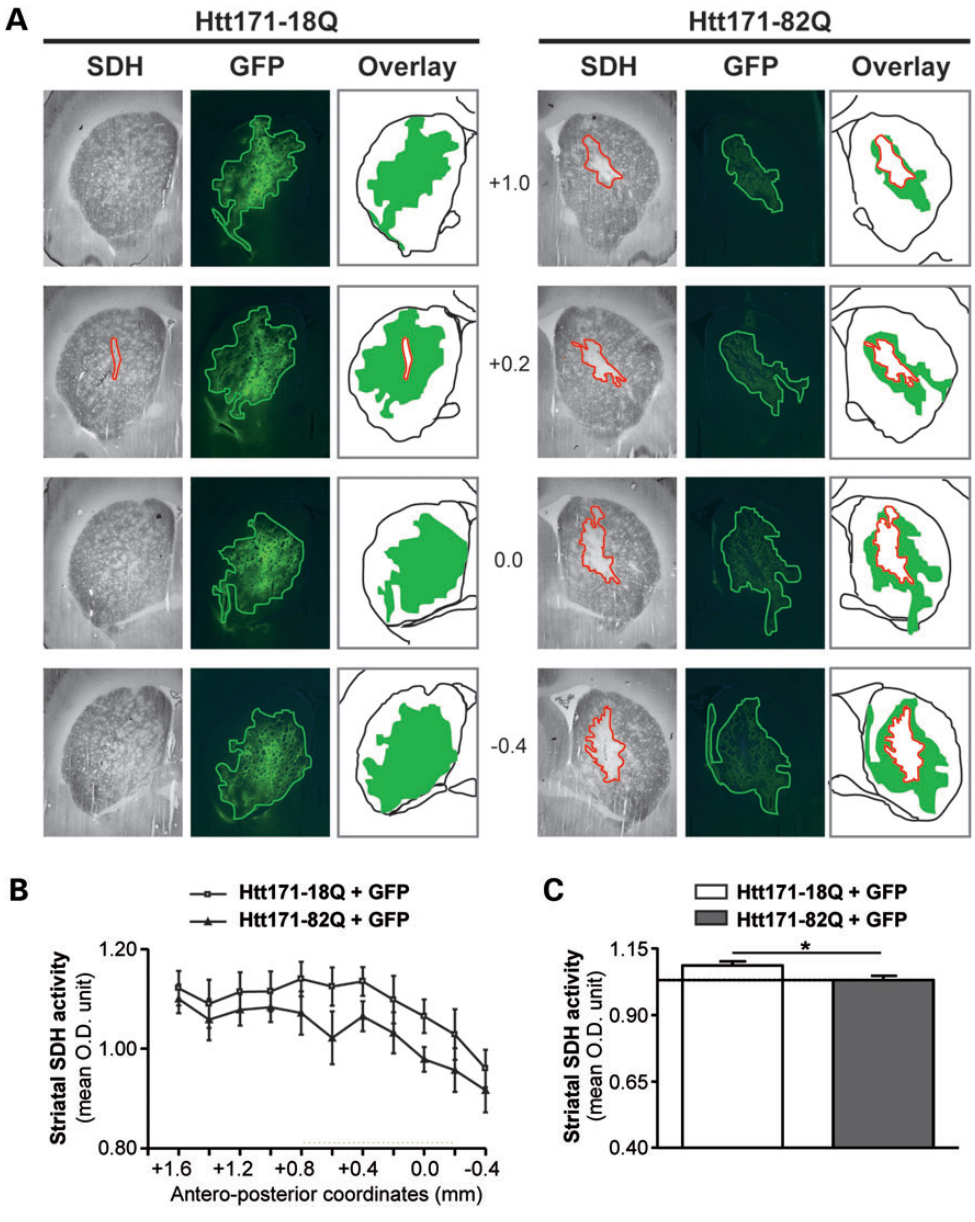

Figure 4. Lentiviral vectors expressing mHtt fragment leads to a loco-regional reduction in SDH activity *in vivo*. Animals were infected with a mixture of lentiviral vector encoding the reporter fluorescent protein GFP mixed with vectors coding Htt171-18Q (left panel) or mHtt171-82Q (right panel). (**A**) Bright field (SDH histochemistry) or fluorescence images were taken from representative coronal brain sections at the levels of the striatum at 6 weeks post-infection. Red lines delineate areas of SDH activity loss. Overlay show the area of SDH loss (red) superimposed to area where the transgenes are expressed (green). Note minimal loss of SDH activity in the control group, in contrast to the striatum injected with lenti-Htt171-82Q. Note that the zone presenting the loss of SDH activity is within the area expressing mHtt. (**B**) Analysis of the total SDH activity in the striatum along the rostrocaudal. (**C**) Histograms corresponding to the total SDH activity measured in the striatum in both groups. Scale bar, 1 mm. Data are expressed as the mean ± SEM. $^{*}P < 0.002$, $n = 6$ per group, two-way ANOVA and *post hoc* Bonferroni/Dunn test.

analysis. We found in a first series of experiments that SDH activity was clearly reduced in the striatum of rats at 8 weeks after infection with lenti-Htt171-82Q. To more precisely characterize this phenomenon of SDH loss and determine whether it could occur earlier in our model, we co-infected the striatum with a mixture of lenti-Htt171-82Q plus lenti-green fluorescent protein (GFP) or a mixture of lenti-Htt171-18Q plus lenti-GFP and examined the animals at 6 weeks post-infection. The injection of lentiviral vectors coding for GFP allowed us to precisely delineate the area that was infected using fluorescence detection [i.e. expressing mHtt or wild-type Htt (wt-Htt)] on frozen sections (Fig. 4). Thus, we could determine whether the area presenting a reduction in C-II activity as seen using SDH histochemistry could be superimposed on that expressing mHtt and GFP. Microscopy observation indeed indicated that the area of SDH loss co-localized within the area of GFP as seen on adjacent sections when lenti-Htt171-82Q was co-injected (Fig. 4). In contrast, when lenti-Htt171-18Q was co-injected with lenti-GFP, there was no loss of SDH activity (Fig. 4). We performed semi-quantitative analysis of the average SDH activity of the striatum along its rostro-caudal extension after infection with lenti-Htt171-82Q in comparison with SDH activity measured

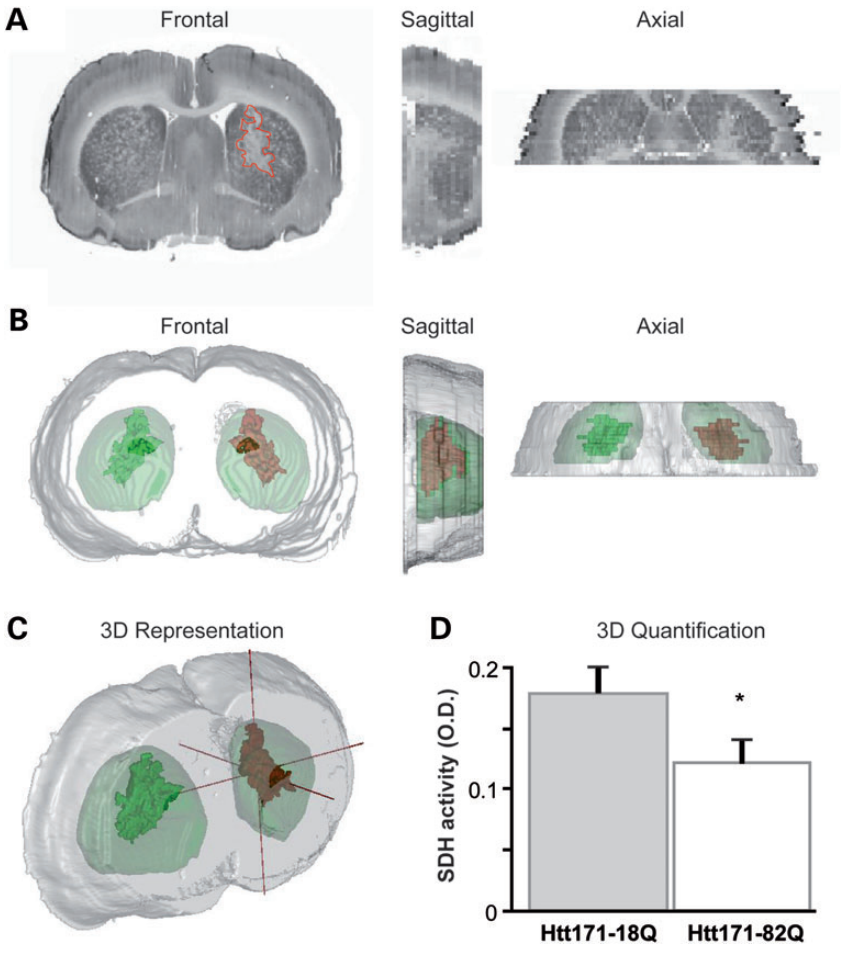

Figure 5. Estimation of the loss of SDH activity in the area expressing mHtt in the lentiviral rat model. (**A**) Bright field (SDH histochemistry) or fluorescence images were taken from representative coronal brain sections at the levels of the striatum at 6 weeks post-infection and stacked for 3D reconstruction. (**B** and **C**) 3D reconstruction of the brain anatomy (gray) with super-imposition of the volume presenting a loss of C-II activity (red) in the striatum infected with lenti-Htt171-82Q (mHtt) and its symmetrical projection in the striatum with wt-Htt (green). (**D**) Histograms corresponding to the regional SDH activity measured in the striatum expressing Htt171-82Q and symmetrically in the contra-lateral striatum. Scale bar, 1 mm. Data are expressed as the mean ± SEM. $^{*}P < 0.01$, $n = 6$ per group, paired Student's *t*-test.

in the contralateral striatal area infected with lenti-Htt171-18Q. Analysis showed that the loss produced by Htt171-82Q was highly significant (two-way ANOVA; Htt171-82Q effect, $F = 4.82$, $P < 0.03$; Antero-posterior levels, $F = 9.12$, $P < 0.003$, and *post hoc* Bonferroni/Dunn test, $P < 0.0017$), although of minimal amplitude (~10%), since the volume of infection was small compared with the entire striatum (Fig. 4). In order to better characterize the loss of SDH activity, tridimentional (3D) reconstruction was performed to measure SDH activity in the area of depletion in the striatum infected with lenti-Htt171-82Q and automatically compared with the activity in the contralateral striatum injected with lenti-Htt171-18Q as a control. A statistically significant ~30% loss of SDH activity was found (group, *n*, mean ± SEM; lenti-Htt171-18Q, $n = 6$, 0.180 ± 0.007 OD unit; lenti-Htt171-82Q, $n = 6$, 0.125 ± 0.006 OD unit; $P < 0.01$, paired Student's *t*-test). Thus, the expression of mHtt produces a severe loss of C-II activity *in vivo* (Fig. 5).

We next took advantage of the ability to detect GFP on fresh tissue to prepare tissue extracts containing mostly striatal neurons expressing Htt171-82Q or Htt171-18Q after infections. Small punches were made in the GFP-positive area on fresh slices and processed for western blot analysis. We assessed the level of expression of the C-II subunit, Ip and Fp at 6 weeks post-infection using western blot analysis (Fig. 6). Extracts from striata infected with lenti-Htt171-82Q displayed similar actin levels when compared with lenti-Htt171-18Q (group, *n*, mean ± SEM; lenti-171Htt-18Q, $n = 6$, 2.52 ± 0.27 OD unit; lenti-Htt171-82Q, $n = 6$, 2.79 ± 0.37 OD unit; unpaired Student's *t*-test, $P > 0.58$), consistent with equal protein loading and the absence of major neurotoxic effects of mHtt at these early time points after infection. The levels of the Core2 subunit of complex III showed no change between groups, indicating that mitochondria density was not markedly changed in the HD context (not shown). The expression of the Ip protein, however, was significantly reduced at 6 weeks post-infection in the samples expressing Htt171-82Q (Ip/actin ratio; lenti-Htt171-18Q, $n = 6$, 0.275 ± 0.037; lenti-Htt171-82Q, $n = 6$, 0.142 ± 0.033; unpaired Student's *t*-test, $P < 0.02$). The expression of the Fp subunit showed a trend to decrease that did not reach significance

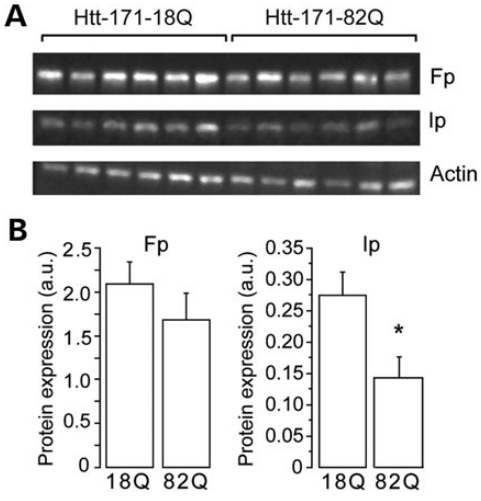

Figure 6. Loss of C-II subunits produced by mHtt in the rat lentiviral model. Rats were infected with a mixture of lentiviral vector encoding the reporter fluorescent protein GFP mixed with vectors coding either Htt171-18Q (left panel) or mHtt171-82Q (right panel). Small striatal samples expressing mHtt or wt-Htt were dissected out at 6 weeks and analyzed by western blotting. Equal amount of proteins was loaded in each lane. Each lane represents a different rat. (**A**) A typical western blot of samples obtained at 6 weeks post-infection showing expression of Fp, Ip and actin in striatal samples. (**B**) Histograms corresponding to the quantification of the expression of the proteins by image analysis. Note that there is a significant loss of SDH subunit Ip, while only a trend is seen for the Fp subunit. Results are the mean ± SEM. $^{*}P < 0.02$, $n = 6$ per group, unpaired Student's *t*-test.

(Fig. 6; Ip/actin ratio: lenti-Htt171-18Q, $n = 6$, 2.091 ± 0.252; lenti-Htt171-82Q, $n = 6$, 1.685 ± 0.304; unpaired Student's *t*-test, $P < 0.02$).

Overexpression of Ip and Fp C-II subunits is neuroprotective against mHtt *in vivo*

To test whether the loss of C-II subunits might play a causal role in mHtt toxicity *in vivo*, we examined whether the overexpression of subunits could be neuroprotective. We attempted to overexpress the subunits of C-II *in vivo* using lentiviral vectors as we previously did in cell cultures (17,18). The lentiviral constructs coding for C-II Ip and Fp were similar to those used for *in vitro* experiments but were prepared at higher titres for *in vivo* infections. Batches of lenti-Fp and lenti-Ip vectors were first re-tested in primary cultures of striatal neurons to show that they indeed induced an increased expression of Fp and Ip proteins (not shown). For the *in vivo* experiments, the same batches of vectors coding C-II subunits were mixed with lenti-GFP and injected into the striatum. Four weeks later, striatal punches were made in the GFP-positive area and analyzed by western blotting. Results showed that levels of the Fp subunit were significantly increased in the area infected with lenti-Fp (Fig. 7A). Ip levels in the striatum infected with lenti-Fp were not modified. After the infection with lenti-Ip, the levels of the Ip subunit were increased, while the Fp levels remained unchanged (Fig. 7B). Using the same experimental paradigm, we tested histoenzymatically on frozen sections from other infected animals, if the activity of C-II was increased in the striatal area where the lenti-Fp or lenti-Ip was injected. Results showed that Fp or Ip overexpression produced no major increase in

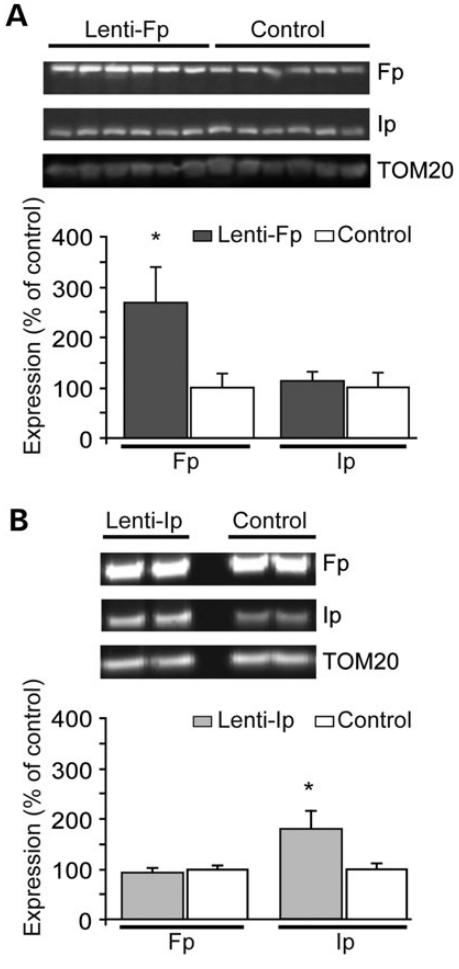

Figure 7. Study of the transduction efficacy of lentiviral vectors coding C-II Ip and Fp subunits *in vivo*. Rats received intrastriatal injection of lenti-Fp (**A**) and lenti-Ip (**B**) mixed with lenti-GFP and the infected area was dissected out 4 weeks later using fluorescence detection for western blot analysis. Representative western blots are shown in upper panel. Control rats have been injected with lentiviral vectors coding the reporter gene LacZ. Results are the mean ± SEM. $^{*}P < 0.01$, $n = 4–6$ per group, unpaired Student's *t*-test.

SDH activity (group, *n*, mean ± SEM; lenti-Fp: $n = 3$, 0.798 ± 0.051 OD unit; lenti-Ip, $n = 3$, 0.754 ± 0.021 OD unit; lenti-LacZ (control), $n = 4$, 0.782 ± 0.009 OD unit; one way ANOVA, n.s., $P > 0.6$) (Supplementary Material, Fig. S1).

We next examined the potential neuroprotective effects of lenti-Fp or lenti-Ip against lenti-Htt171-82Q toxicity. In these neuroprotection experiments, lenti-GFP was used as a control of viral load for infection. After 12 weeks, as expected based on previous works (25–28), infection of the striatum with lenti-Htt171-82Q produced local degeneration characterized by loss of DARPP-32 immunohistochemical labeling and COX histochemical labeling (Fig. 8). In the case of the infection with lenti-Htt171-18Q, no major lesion was observed except for the small mechanical trauma produced by the needle during the stereotaxic injection of viral suspensions. The volume of the loss of DARPP-32 and COX produced by lenti-Htt171-18Q was minimal (mean ± SEM; $n = 10$; DARPP-32: 0.075 ± 0.013 mm^3; COX: 0.054 ± 0.019 mm^3). Infection with lenti-Htt171-82Q mixed with lenti-GFP produced much larger lesions readily detected under

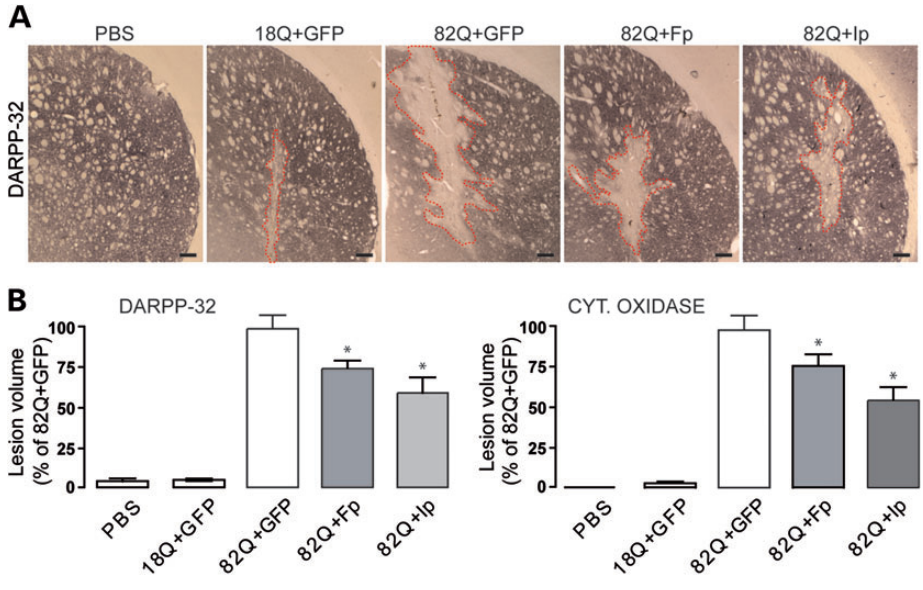

Figure 8. Neuroprotective efficacy of Fp and Ip against mHtt neurotoxicity *in vivo*. Rats were co-injected with lentiviral vectors encoding wt-Htt171-18Q fragment or mHtt171-82Q plus either, Fp, Ip or GFP as a control of viral load. Rats were killed at 12 weeks post-surgery and processed for histological evaluation. (**A**) Photomicrographs of representative lesions seen in the different groups of rats o characterize striatal degeneration using DARPP-32 immunohistochemistry. Scale bar, 200 μm. Histograms in (**B**) represent the volume of lesions produced in the different conditions when assessed by the Cavalieri method using DARPP32 immunohistochemistry (left) and cytochrome *c* oxidase (Cyt. Oxidase) histochemistry (right). Note that the volume of striatal lesions produced by mHtt is significantly reduced by overexpressing Fp and Ip proteins when compared with control (GFP). Data are the mean ± SEM. $^{*}P < 0.01$, $n = 10–12$ per group, one-way ANOVA followed by the Bonferroni *post hoc* test.

microscope observation ($n = 9$; DARPP-32: 1.550 ± 0.115 mm^3; COX: 1.855 ± 0.132 mm^3). Co-infection with lenti-Htt171-82Q mixed with lenti-Fp produced a partial (~30%) but significant reduction in the volume of striatal lesions produced by lenti-Htt171-82Q plus lenti-GFP as seen using DARPP-32 and COX staining (Fig. 8) ($n = 10$; DARPP-32: 1.159 ± 0.080 mm^3; COX:1.433 ± 0.137 mm^3; $P < 0.002$ and $P < 0.02$, respectively, when compared with lenti-Htt171-82Q+lenti-GFP, ANOVA and the *post hoc* Bonferroni test). Co-infection with lenti-Ip produced a stronger (~50%) reduction in the mHtt-induced lesion compared with control (Fig. 8) ($n = 12$; DARPP-32: 0.917 ± 0.145 mm^3; COX: 1.008 ± 0.144 mm^3; $P < 0.005$ and $P < 0.004$, respectively, when compared with lenti-Htt171-82Q+lenti-GFP, ANOVA and the *post hoc* Bonferroni test). Thus, the overexpression of Fp and Ip is neuroprotective against mHtt toxicity.

We also examined whether the overexpression of the Ip subunit could have an effect on mHtt-containing aggregates. The number and the size of aggregates detected by EM48 immunohistochemistry in rats infected with lenti-Htt171-82Q were not significantly different between rats co-infected with lenti-Ip and animals infected with lenti-GFP. This indicated no major effect of Ip overexpression on mHtt aggregation (Supplementary Material, Fig. S2).

DISCUSSION

The present study shows that the assembly of C-II in the mitochondria is defective in the N171-82Q transgenic mouse model of HD expressing the N-terminal part of mHtt. This is accompanied by a reduction in mitochondrial biogenesis. Decreased assembly of C-II corresponds to a reduced activity, as seen by oxygen consumption assays. We also show that the expression on the Ip subunit of C-II is significantly decreased in two different genetic models expressing short N-terminal fragments of mHtt. Moreover, we show that the overexpression of the C-II subunit Fp protein and, more efficiently, the Ip protein can prevent mHtt-induced degeneration of striatal neurons *in vivo*.

The N171-82Q mouse models we examined indicated that the assembly of C-II was defective at relatively early stage of the disease. Indeed, loss of C-II assembly was observed at 1 month of age in these HD mice expressing an expanded polyQ tract when compared with transgenic mice expressing the wild-type fragment with 18 glutamines. At this early time point, the expression of the other mitochondrial complexes appears unchanged when compared with controls. Later, BN-PAGE analysis showed that the C-II levels were persistently low and that the C-IV levels in the respiratory chain were also found to be reduced. The results obtained by BN-PAGE functionally corresponded to the results obtained by the classic respirometry assays. Reduced assembly of C-II in N171-82Q mice is followed by a reduction in the activity of the complex. Indeed, oxidative phosphorylation/O_2 consumption evaluated using succinate as a substrate was significantly decreased in N171-82Q mice. Consistent with C-II defects, we found that the total levels of the Ip protein are reduced in the striatum of a different mouse model, the R6/1 line at 16 weeks of age, an early stage in these mice that die around 30–35 weeks (29). Western blot analyses showed that the loss of Ip is relatively selective, since the levels of the Fp subunit are not significantly reduced in this mouse model. A loss of C-II activity along with a preferential reduction in Ip subunit levels were also found 6 and 8 weeks after intrastriatal infection in the lentiviral model of HD in rats. This

loss was circumscribed to the striatal region expressing the mHtt fragment. All these observations are congruent with our previous findings in primary cultures of striatal neurons expressing mHtt, where loss of Ip preceded that of Fp (17), and was seen while many other mitochondrial proteins showed no major expression changes. Thus, the present observations are compatible with the possibility that the relatively selective reduction in the expression and incorporation of the Ip protein in the C-II at the level of the respiratory chain could lead to a general reduction in the assembly and/or the stability of C-II and partial loss of its activity. Other studies reported preferential defects in C-II in Yeast (23) and mammalian cell models expressing mHtt exon 1 (30). Interestingly, transient changes in Ip subunit expression in R6/2 mice have been described using a careful a large scale proteomic analysis of the forebrain, with very early reduction in the expression at 2 and 8 weeks of age (20). Such changes were not seen in other studies in R6/2 mice, while C-II activity tended to increase at early stage of the disease in YAC72 mice (31).

The defects in C-II have been consistently observed in the striatum of HD patients. Enzymatic activity of C-II was preferentially reduced in the striatum of symptomatic patients, while the cerebral cortex showed no significant modifications (15,16,32–36). Indications of C-II defects were also reported in muscle from HD patients (37). The expression of the Ip protein is markedly reduced in the caudate and putamen of symptomatic HD patients, while the expression of many other mitochondrial proteins remains essentially normal (17). Importantly, the loss of the Ip protein was found to occur preferentially in the striatum, while no significant reduction in expression could be observed in the cerebral cortex and cerebellum of HD patients. A similar regional analysis of the C-II assembly using BN-PAGE could not be carried out in N171-82Q mice, since the method requires too much material for mitochondria preparation. However, the present western blot analysis of the striatum of R6/1 mice showed a significant reduction in the total levels of Ip (assembled and not assembled). Thus, it is possible that the loss of the C-II assembly and activity and a reduction in Ip expression are phenomena that preferentially affect the striatum.

The relationship between the different changes we observed (Ip loss, C-II assembly defects, reduced C-II activity) is not yet totally elucidated in terms of causality. The elucidation of the mechanisms that could mediate the down-regulation of Ip awaits further studies. A few working hypotheses have been already discussed previously (17). The present observations suggest that it may be a consequence of defective assembly mechanisms leading to an increase in the rate of degradation of the protein.

The defects in C-II may result from a mHtt-induced dysfunction of mitochondria. In the present study, we observed a reduction in mitochondrial biogenesis in N171-82Q mice. This is consistent with the functional alteration of the PGC-1α pathway in HD (14). PGC-1α is a co-activator of transcription that plays a key role in stimulating mitochondrial biogenesis through its action on the transcription factors NRF-1 and NFR-2 (38,39). NRF-1 activates the transcription of mitochondrial genes, such as COX1 and cytochrome *c*. A well-documented study showed that the promoter of the SDH-B gene encoding for the Ip subunit has functional sites that bind NRF-1 and NRF-2 in the proximity of the initiation site (40). However, the hypothesis that the loss of PGC-1α is directly responsible for the loss of C-II is not compatible with the observation that levels of mRNA coding SDH-Ip or SDH-Fp are not changed in HD patients and models. Our *in vitro* study on striatal neurons showed unchanged levels of the SDH-Ip mRNA, while levels of the Ip protein were down regulated (17). In line with this, SDH-Ip (and SDH-Fp) mRNA levels are not markedly reduced in HD patients and mouse models as assessed by gene arrays studies (41,42), while enzymatic C-II activity and Ip levels are down regulated. Similarly, whereas SDH-Ip mRNA expression is not changed in R6/2 mice, levels of the protein vary depending on the age of the mice (20). Thus, Ip regulation likely occurs at a post-transcriptional level.

One possible post-transcriptional regulatory mechanism of Ip expression may be linked to the well-documented alterations of mitochondrial membrane potential in HD (1). This could disturb the import of C-II constituents, since the machinery of protein import uses mitochondrial membrane potential (43).

The defects in the C-II assembly may also result from the alteration of specific molecular factors for import/assembly of Ip into the complex. Destabilization of the C-II assembly may more profoundly alter the levels of Ip when compared with the other subunits of the complex. The proteins involved in the import of Ip and more generally C-II subunits have not been identified in mammals. The protein coded by TCMP62 in Yeast likely codes a chaperone-like protein involved in the C-II assembly (44,45). It is a membrane protein that interacts with SDHA and SDHB gene products. Knockdown of TCMP62 leads to the loss of the C-II assembly. There is no known homolog in mammals. SDH Assembly Factor 1 (SDHAF1) has been recently found to be key SDH assembly factor (46). Other few proteins have been identified to interact with Ip and Fp proteins, including human Frataxin and its Yeast ortholog Yfh1p (47) and the protein CART (cocaine- and amphetamine-regulated transcripts) which is neuroprotective in cell models of ischemia/hypoxia (48).

Post-transcriptional modification of the C-II subunit may also regulate the C-II assembly. The C-II/SDH subunit Fp has been shown to be regulated by acetylation. Recent experiments showed that Fp is hyperacetylated in SIRT3 knockout mice and SIRT3 directly deacetylates Fp in a nicotinamide adenine dinucleotide (NAD)-dependent manner (49,50). Fu and collaborators demonstrated that mHtt leads to a decrease in SIRT3 activity (51). This may be a consequence of both reduced PGC-1α as well as reduced NAD concentrations. Thus, loss of SIRT3 in the HD context may lead to hyperacetylation of Fp, reducing the assembly of Fp in C-II, perturbing the turnover of Ip and eventually decreasing the enzymatic activity of C-II. A loss of SIRT3 has been implicated in other neurodegenerative diseases including Friedriech ataxia (52).

One important finding in the present study is that the overexpression of the SDH Ip subunit, and to a lesser extent, SDH Fp exerts significant neuroprotective effects against mHtt *in vivo*. This indicates, as suggested by our previous *in vitro* experiments, that loss of Ip in HD models may contribute to neurodegeneration. This protective effect may appear at first surprising, since loss of Ip is likely not an early event in the molecular cascade triggered by mHtt to kill neurons. Especially, the reduced expression of PGC-1α, mitochondrial biogenesis, altered mitochondrial membrane potential, abnormal fragmentation and cristae disorganization are likely preceding C-II loss and reduction in Ip

levels. However, neurodegeneration signaling might be seen as a non-linear phenomenon rather resembling to a vicious cycle. Overexpression of Ip (and similarly Fp) likely produces a stabilization of C-II levels which may have important consequences to maintain energy production in the tricarboxylic acid (TCA) cycle and electron flow in the respiratory chain. Ip may also contribute to control reactive oxygen species (ROS) production as suggested by others, since the Ip protein is considered to be a potential 'sensor' of the ubiquinone pool in the mitochondria (53). Although C-II is debated as a source of ROS by itself, compelling evidence showed that disturbing C-II function at least indirectly produces the elevation of ROS levels, and increased ROS production is a well-documented feature of both HD transgenic mice and HD patients (54). Thus, the overexpression of Ip and the improved stabilization of C-II may be sufficient to delay striatal neuron demise. Our data suggest that while important contributors of mHtt -induced energy perturbation (e.g. perturbation of PGC-1α) are upstream of the deregulation of C-II by mHtt, the consequent loss of the Ip protein is a key event contributing to the expression of neurodegeneration and that correcting this anomaly retards the death/dysfunction of striatal neurons.

The lentiviral gene transfer approach for the overexpressing Ip protein should be so far considered as only a proof of principle that *in vivo*, C-II may be an interesting therapeutic target for slowing degeneration in HD. It would be of prime interest to find small molecules that could increase Ip expression and C-II stabilization or anaplerotic chemicals that bypass C-II defects or improve TCA cycle and respiratory chain efficiency. Other potential approaches would be to utilize agents which increase the expression of PGC-1α (e.g. bezafibrate) or which improve mitochondrial function as recently shown using the mitochondrial anti-oxidant XJB-5-131 (55,56). The results provide further evidence that targeting mitochondrial dysfunction in HD may be a useful therapeutic strategy.

MATERIALS AND METHODS

Animals

Rats

Four-month-old male Sprague-Dawley rats (Charles River) were used. The animals were housed in a temperature-controlled room maintained on a 12 h light/dark cycle. Food and water were available ad libitum. Experiments were performed in accordance with the European Community Council directive 86/609/EEC for the care and use of laboratory animals or were approved by the Animal Care and Use Committee of the Weill Medical College of Cornell University.

Transgenic mice

Transgenic mice expressing the wt-Htt (N171-18Q) and mHtt (N171-82Q) N-terminal fragment of the human Htt (22), as well as non-transgenic littermates were obtained from the Jackson Laboratory (Bar Harbor, ME, USA) and bred at the Weill Medical College of Cornell University animal facility. Both male and female mice expressing wt-Htt or mHtt were studied at various disease stages and compared with non-transgenic age- and gender-matched littermates. In most experiments, a similar number of male and female pairs were used. In these mice, the symptomatic stage is characterized by incoordination, ataxia and weight loss with onset at ∼3 months of age. Mice die prematurely at ∼6 months of age. Male R6/1 transgenic mice expressing exon-1 of human mHtt were obtained from Jackson Laboratory. Mice were genotyped by PCR as described previously (21). Animals were bred at the animal facility of the University of Barcelona. R6/1 mice were used when they started to have motor coordination impairment at 16 weeks of age (29).

Isolation of brain mitochondria

Non-synaptic brain mitochondria were isolated by a Percoll^{TM} gradient purification method as described previously (57). All procedures were conducted at 4°C. Mice were sacrificed by decapitation and the forebrain was excised and homogenized in a mannitol-sucrose isolation medium (225 mM mannitol, 75 mM ultrapure sucrose, 5 mM *N*-2-hydroxyethylpiperazine-*N*′-2-ethanesulfonic acid (HEPES), pH 7.4) containing 0.1 mg/ml fatty acid-free bovine serum albumin (BSA) and 1 mM ethylene glycol tetraacetic acid (EGTA). Homogenates were centrifuged for 6 min at 2400*g* in a Beckmann L8-80 ultracentrifuge using a 50 TI rotor. The supernatant was collected and centrifuged for 14 min at 13 000*g*. The resulting pellet was resuspended in isolation medium containing 15% Percoll^{TM} and 1 mM EGTA and layered on the top of a discontinuous Percoll^{TM} gradient (23/40%). The gradient was centrifuged for 14 min at 38 000*g*, and the 23/40 inter-phase layer, containing the mitochondria, was collected. Mitochondria were washed three times with isolation medium without BSA and centrifuged for 14 min at 13 000*g*. The pellet containing purified mitochondria was resuspended in 100 μl of isolation buffer without EGTA and BSA (58). Mitochondrial protein concentration was measured with a protein assay kit (BioRad, Hercules, CA, USA), using BSA as a standard.

Blue native PAGE

We have investigated by blue native gel electrophoresis the molecular organization of the mitochondrial respiratory chain.

BN-PAGE is a high-resolution electrophoretic technique used for the isolation of membrane bound proteins (59). The solubilization of biological membranes in cellular or mitochondrial preparations is obtained by applying mild detergents. Upon the addition of the coomassie dye (Coomassie blue G-250) protein aggregation is reduced, all the membrane proteins, and also many water soluble, acquire a negative charge which pulls to the anode during electrophoresis, irrespectively of their isoelectric point.

Fifty micrograms of the brain mitochondrial preparation were resuspended in 50 μl of a BN mitochondria buffer (1.5 M aminocaproic acid, 50 mM bis–tris, pH 7.0, at 4°C) and then treated with 2 μl of *N*-dodecylmaltoside (DDM; 10% w/v) on ice for 5′. Finally, samples were centrifuged for 30 min at 20 000*g*. The supernatants were transferred to clean tubes and 5 μl of a BN sample buffer (Coomassie Blue G-250 5% w/v suspension in 750 mM 6-aminohexanoic acid, 50 mM bis–tris, 0.5 mM ethylenediaminetetraacetic acid, pH 7.0, at 4°C) was added to the samples for BN-PAGE. Gels were cast as described for BN-PAGE (60,61). We used 5–13% acrylamide gradient gels with 4% sample gels on the top to separate DDM-solubilized individual mitochondrial complexes. Gels were run in a vertical

electrophoresis apparatus under the conditions described for BN-PAGE (61). Transfer of proteins onto a polyvinylidene difluoride (PVDF) membrane (Amersham Biosciences) was carried out overnight at 30 V at 4°C. For immunodetection of protein complexes, monoclonal antibodies (Molecular Probes) against the following subunits were used: 39 kDa of complex I, 70 kDa of complex II, core 2 of complex III, subunit I of complex IV and subunit β of complex V. Native high molecular weight markers were from Amersham Biosciences (59). For protein loading control, the 10 μl of the DDM-treated mitochondrial preparation was mixed to an equal amount of Laemmli sample buffer and loaded in an SDS–PAGE. Transfer onto a PVDF membrane was carried out as described above. Outer (TOM20) or inner (TIM 23) membrane markers were immunodetected with a specific antibody (Santa Cruz). When the antibody against the 70 kDa (Fp) subunit was used, a reserve pool of the not assembled 70 kDa subunit was immunodetected as a second and lower molecular weight band in addition to the fully assembled C-II band, normally detected around 130 kDa. Depending on the daily hand-cast gradient gel preparation and the bands migration, this protein would go undetected when co-migrating with the Brilliant blue G in the dye front. Brain mitochondria isolated from five animals of each genotype and age group were compared as shown.

Oxygen consumption

The rate of O_2 consumption was measured in brain mitochondria using a Clark oxygen electrode in a waterjacketed cell, magnetically stirred at 37°C (Hansatech Instruments, Norfolk, UK) as previously described (62,63). Briefly 10 μl of freshly isolated brain mitochondria was resuspended in a respiration medium (125 mM KCl, 20 mM HEPES, 1 mM $MgCl_2$, 2 mM KH_2PO_4, pH 7.4). State 3 respiration was recorded in the presence of 0.4 mM adenosine di-phosphate. The state 3 rates were recorded in the presence of glutamate:malate 5:1 mM or glutamate:succinate 5:2 mM. State 4′ was induced with the specific inhibitor of the Adenine Nucleotide Translocator, carboxy Atractilate. The protein content in all samples was measured with a protein assay kit (BioRad), using BSA as a standard. For oxygen consumption, the comparison between wild-type and Tg was done day by day to minimize variability due to isolation. Brain mitochondria isolated from six animals of each genotype and age group were compared.

Quantitative real-time PCR

For the quantification of the relative amount of mitochondrial DNA (mtDNA), total DNA was isolated from liquid nitrogen frozen striatal sections of transgenic (N171-18Q and N171-82Q), as well as non-transgenic mice, as described (64). The mtDNA copy number was determined by qRT-PCR using SYBR Green Chemistry on a Roche Light Cycler (Roche, USA). The abundance of the mtDNA-encoded template [from nucleotide (nt) 6409 to nt 6636] in the COX1 gene sequence was assayed (primers: forward CAT CCC TTG ACA TCG TG, reverse CTG AGT AGC GTC GTG G) and normalized using a nuclear-encoded template for the 18S gene (primers: forward CGGACAGGATTGACAGA, reverse: CCAGTCAGTGTAGCGC) (65). Each reaction was optimized and confirmed over an appropriate linear concentration range using genomic DNA standards. Samples were analyzed in duplicate for both assays, enabling the calculation of the average mtDNA:nuclear DNA ratio. The numbers of samples for these experiments were as follows: for N171-82Q, $n = 7$ at 1 and 2 months, $n = 5$ at 3 months and $n = 6$ at 4 months; for N171-18Q: $n = 6$ at 1 and 2 months of age and $n = 11$ at 3 and 4 months of age.

Lentiviral vector production and intrastriatal injection

Vector production

The construction of SIN-W-PGK (mouse phosphoglycerate kinase 1) vectors encoding Htt171-18Q and Htt171-82Q has been described previously (26), as has the GFP construct (66). Construct for overexpressing Fp and Ip proteins have been also described previously (17,18). Viral particles were produced in human embryonic kidney 293 T cells using a four-plasmid system (67), collected by ultracentrifugation and suspended in phosphate-buffered saline (PBS) with 1% BSA. The particle content of the viral batches was determined by enzyme linked immunosorbent assay for the p24 antigen (Gentaur, France). Viral particles were used at a concentration of 200 000 ng of p24 per μl in 0.1 M PBS with 1% BSA for intrastriatal injections.

Stereotaxic injection

Rats were anesthetized with ketamine/xylazine (75 and 10 mg/kg, respectively; i.p.) and placed in a stereotaxic frame. Bilateral stereotaxic injections into the striatum were made using a 30 gage blunt-tip steel needle connected to a 10 μl Hamilton syringe (Hamilton, Reno, NV, USA) via a 30 cm polypropylene catheter. Viral suspensions from the same batch were injected into each striatum at 0.25 μl/min by means of an automatic injector (Stoelting, Wood Dale, IL, USA), using the following coordinates: 0.8 mm rostral to bregma, 3.5 mm lateral to midline and 4.0 mm ventral to the skull surface, with the tooth bar set at 3.3 mm (27). At the end of the injection, the needle was left in place for 5 min, before being slowly withdrawn.

Brain tissue processing for histological evaluation and biochemical analysis in rats

Histological evaluation

Rats received an overdose of sodium pentobarbital and were transcardially perfused with phosphate buffer containing 4% paraformaldehyde (PFA). Brains were then post-fixed in 4% PFA for 24 h and then cryoprotected by immersion in 15 and 30% sucrose for 48 h. Coronal sections (thickness 40 μm) were cut at −22°C using a sliding microtome (Cryocut 1800; Leica Microsystems, Nussloch, Germany). Free-floating sections encompassing the entire striatum were serially collected and stored in antifreeze cryoprotectant solution at −20°C until immunohistochemical processing. Immunohistochemistry of DARPP-32 (rabbit polyclonal antibody, Chemicon Intl. Inc., diluted 1:5000) and immunohistochemistry of EM48 (mouse monoclonal antibody, MAB5374, Chemicon Intl. Inc., diluted 1:1000) were performed as described previously (27). Immunoreactivity was revealed using the Vectastain ABC Elite System (Vector, Burlingham, CA, USA). The sections were mounted, dehydrated by passing through ethanol and toluene and

coverslipped with Eukitt. COX histochemistry was performed as previously described according to the method of Wong-Riley (68).

Determination of striatal DARPP-32-and COX-depleted volume
The volume of the striatum exhibiting a depletion of DARPP-32 staining was estimated as follows (27,28,69). The unstained area of all serial striatal sections (400 μm apart) was manually delineated using a 4× objective and an AX70 microscope (Olympus, Munster, Germany) coupled with an image analysis system. The volume was then calculated according to the principle of Cavalieri using the formula: volume = d(a1 + a2 + a3 + …), where d is the distance between serial sections (400 μm), and a1, a2, a3 etc. stand for the area showing loss of DARPP-32 immunoreactivity or loss of COX activity ('lesion') within individual serial sections throughout the striatum.

Determination of aggregate numbers
The number of EM48-positive inclusions was quantified as previously described (27) with the following modifications: the inter-section distance was 400 μm (i.e. one in every 10 sections was used) and observations were performed using a 10× objective on a Leica DM6000 microscope equipped with a motorized stage and an automated image acquisition and analysis system (Mercator Software, Explora Nova, La Rochelle, France). With this set-up, objects with an apparent cross-sectional area >3 μm^2 (i.e. diameter > ∼1.1 μm) could be reliably detected. Counting and determination of cross-section areas of aggregates were determined for ∼6000–12 000 EM48-positive objects per striatum (i.e. 5–9 sections) in 8 rats/group.

SDH histo-enzymatic assay
Animals received an overdose of sodium pentobarbital and the brain was removed and frozen in −25°C isopentane and stored at −80°C. Coronal frozen sections (thickness 20 μm) were cut at −20°C using a cryostat (3035S, Leica Microsystem). Histochemical revelation of SDH activity was performed as described previously (69,70). Succinate was used as the specific substrate, and nitro blue tetrazolium (NBT) was used as electron acceptor, which eventually forms formazan. Serial brain sections were first incubated for 10 min in 0.1 M phosphate buffer and 0.9% NaCl (PBS) at 37°C to activate SDH, which is substantially inactivated by tightly bound oxaloacetate (71). Sections were then rinsed in a large volume of PBS and immersed in the reaction medium containing 5 mM NBT, 0.05 M phosphate buffer (pH 7.6) 0.05 M sodium succinate for 40 min at 37°C. Sections were then rinsed in cold PBS for 5 min, immersed for few seconds in deionized water and air-dried at room temperature. During the staining procedure, care was taken to avoid sunlight, which degrades NBT.

SDH activity analyses
Semi-quantitative analysis of SDH activity in the entire striatum was performed using densitometry analysis (using MCID software) as described previously (69,70). In the case of the analysis of the entire striatum, 8–10 animals per group were examined. For subregional analysis of SDH activity in the striatum based on the visualization of the expression of GFP, acquired image of SDH-stained section was aligned with the adjacent section imaged for GFP fluorescence using a Zeiss Axioplan2 Imaging microscope, a ×1.25 objective and cooled CCD camera and an image acquisition and analysis system (Mercator, Explora Nova). For each animal, region of interest was delineated on the GFP images (5–12 sections, 200 μm interspace), pasted and translated to be located at the same anatomical level on the SDH image for the determination of optical density in the region. The mean ± SEM SDH OD unit in the GFP-containing area was calculated from all animals. For these analyses, three to four animals were studied in each group.

3D reconstruction of SDH activity
Images of serial sections revealed for SDH histochemistry were digitized using a flatbed scanner (ImageScanner; GE Healthcare Europe, Orsay, France) with 600 dpi resolution (pixel size 42 × 42 μm^2). 3D post-mortem reconstruction was performed using the in-house BrainRAT software freely available on internet (http://brainvisa.info) based on a propagative co-registration strategy. On all coronal sections (n = 18 serial sections/brain) separated by 200 μm, the loss of staining seen as a palor in the striatum infected with lenti-Htt171-82Q was manually segmented in 3D, and corresponding lateralized areas were symmetrically computed in the control (lenti-Htt171-18Q) striatum. Image processing techniques used were described in previous work (72).

Statistical analysis

All data were expressed as the means ± SEM. Unpaired Student's t-test was used for the comparison between two groups. When more than two groups were compared, a one-way ANOVA with multiple comparisons using the *post hoc* Bonferroni test was carried out using commercially available software (StatView® software, SAS Institute Inc., USA). A two-way ANOVA followed by a *post hoc* Bonferroni/Dunn test was used for the analysis of SDH activity throughout the antero-posterior anatomical extension of the striatum in rats infected with lentiviral vectors. For time-dependent changes in mtDNA levels, data were analyzed by two-way ANOVA (ages/genotypes) and pairwise multiple comparison procedures (Holm-Sidak method). For all statistical tests performed, a probability level of 5% was considered significant.

SUPPLEMENTARY MATERIAL

Supplementary Material is available at *HMG* online.

Conflict of Interest statement. None declared.

FUNDING

This work was supported by the 'Commissariat à l'Energie Atomique et aux Energies Alternatives' (CEA) and 'Centre National de la Recherche Scientifique' (CNRS). This work was initiated thanks to a grant from Hereditary Disease Foundation. L.G. was supported by the Neuropôle de Recherche Francilien and the Fondation pour la Recherche Médicale. L.B. was also supported by the Neuropôle de Recherche Francilien. Funding to pay the Open Access publication charges for this article was provided by CNRS (centre national de la recherché scientifique).

REFERENCES

1. Damiano, M., Galvan, L., Deglon, N. and Brouillet, E. (2010) Mitochondria in Huntington's disease. *Biochim. Biophys. Acta*, **1802**, 52–61.
2. Harper, P.S. (1991) Huntington's Disease. WB Saunders Company Ltd, London.
3. Borrell-Pages, M., Zala, D., Humbert, S. and Saudou, F. (2006) Huntington's disease: from huntingtin function and dysfunction to therapeutic strategies. *Cell Mol. Life Sci.*, **63**, 2642–2660.
4. Myers, R.H., Vonsattel, J.P., Stevens, T.J., Cupples, L.A., Richardson, E.P., Martin, J.B. and Bird, E.D. (1988) Clinical and neuropathologic assessment of severity in Huntington's disease. *Neurology*, **38**, 341–347.
5. Sugars, K.L. and Rubinsztein, D.C. (2003) Transcriptional abnormalities in Huntington disease. *Trends Genet.*, **19**, 233–238.
6. Cowan, C.M. and Raymond, L.A. (2006) Selective neuronal degeneration in Huntington's disease. *Curr. Top. Dev. Biol.*, **75**, 25–71.
7. Bossy-Wetzel, E., Petrilli, A. and Knott, A.B. (2008) Mutant huntingtin and mitochondrial dysfunction. *Trends Neurosci.*, **31**, 609–616.
8. Costa, V. and Scorrano, L. (2012) Shaping the role of mitochondria in the pathogenesis of Huntington's disease. *EMBO J.*, **31**, 1853–1864.
9. Mochel, F. and Haller, R.G. (2011) Energy deficit in Huntington disease: why it matters. *J. Clin. Invest.*, **121**, 493–499.
10. Browne, S.E. (2008) Mitochondria and Huntington's disease pathogenesis: insight from genetic and chemical models. *Ann. N. Y. Acad. Sci.*, **1147**, 358–382.
11. Panov, A.V., Burke, J.R., Strittmatter, W.J. and Greenamyre, J.T. (2003) In vitro effects of polyglutamine tracts on Ca2+-dependent depolarization of rat and human mitochondria: relevance to Huntington's disease. *Arch. Biochem. Biophys.*, **410**, 1–6.
12. Panov, A.V., Gutekunst, C.A., Leavitt, B.R., Hayden, M.R., Burke, J.R., Strittmatter, W.J. and Greenamyre, J.T. (2002) Early mitochondrial calcium defects in Huntington's disease are a direct effect of polyglutamines. *Nat. Neurosci.*, **5**, 731–736.
13. Song, W., Chen, J., Petrilli, A., Liot, G., Klinglmayr, E., Zhou, Y., Poquiz, P., Tjong, J., Pouladi, M.A., Hayden, M.R. *et al.* (2011) Mutant huntingtin binds the mitochondrial fission GTPase dynamin-related protein-1 and increases its enzymatic activity. *Nat. Med.*, **17**, 377–382.
14. Cui, L., Jeong, H., Borovecki, F., Parkhurst, C.N., Tanese, N. and Krainc, D. (2006) Transcriptional repression of PGC-1alpha by mutant huntingtin leads to mitochondrial dysfunction and neurodegeneration. *Cell*, **127**, 59–69.
15. Browne, S.E., Bowling, A.C., MacGarvey, U., Baik, M.J., Berger, S.C., Muqit, M.M., Bird, E.D. and Beal, M.F. (1997) Oxidative damage and metabolic dysfunction in Huntington's disease: selective vulnerability of the basal ganglia. *Ann. Neurol.*, **41**, 646–653.
16. Gu, M., Gash, M.T., Mann, V.M., Javoy-Agid, F., Cooper, J.M. and Schapira, A.H. (1996) Mitochondrial defect in Huntington's disease caudate nucleus. *Ann. Neurol.*, **39**, 385–389.
17. Benchoua, A., Trioulier, Y., Zala, D., Gaillard, M.C., Lefort, N., Dufour, N., Saudou, F., Elalouf, J.M., Hirsch, E., Hantraye, P. *et al.* (2006) Involvement of mitochondrial complex II defects in neuronal death produced by N-terminus fragment of mutated huntingtin. *Mol. Biol. Cell*, **17**, 1652–1663.
18. Benchoua, A., Trioulier, Y., Diguet, E., Malgorn, C., Gaillard, M.C., Dufour, N., Elalouf, J.M., Krajewski, S., Hantraye, P., Deglon, N. *et al.* (2008) Dopamine determines the vulnerability of striatal neurons to the N-terminal fragment of mutant huntingtin through the regulation of mitochondrial complex II. *Hum. Mol. Genet.*, **17**, 1446–1456.
19. Orr, A.L., Li, S., Wang, C.E., Li, H., Wang, J., Rong, J., Xu, X., Mastroberardino, P.G., Greenamyre, J.T. and Li, X.J. (2008) N-terminal mutant huntingtin associates with mitochondria and impairs mitochondrial trafficking. *J. Neurosci.*, **28**, 2783–2792.
20. Zabel, C., Mao, L., Woodman, B., Rohe, M., Wacker, M.A., Klare, Y., Koppelstatter, A., Nebrich, G., Klein, O., Grams, S. *et al.* (2009) A large number of protein expression changes occur early in life and precede phenotype onset in a mouse model for Huntington disease. *Mol. Cell. Proteomics*, **8**, 720–734.
21. Mangiarini, L., Sathasivam, K., Seller, M., Cozens, B., Harper, A., Hetherington, C., Lawton, M., Trottier, Y., Lehrach, H., Davies, S.W. *et al.* (1996) Exon 1 of the HD gene with an expanded CAG repeat is sufficient to cause a progressive neurological phenotype in transgenic mice. *Cell*, **87**, 493–506.
22. Schilling, G., Becher, M.W., Sharp, A.H., Jinnah, H.A., Duan, K., Kotzuk, J.A., Slunt, H.H., Ratovitski, T., Cooper, J.K., Jenkins, N.A. *et al.* (1999) Intranuclear inclusions and neuritic aggregates in transgenic mice expressing a mutant N-terminal fragment of huntingtin. *Hum. Mol. Genet.*, **8**, 397–407.
23. Solans, A., Zambrano, A., Rodriguez, M. and Barrientos, A. (2006) Cytotoxicity of a mutant huntingtin fragment in yeast involves early alterations in mitochondrial OXPHOS complexes II and III. *Hum. Mol. Genet.*, **15**, 3063–3081.
24. Wang, H.Q., Xu, Y.X., Zhao, X.Y., Zhao, H., Yan, J., Sun, X.B., Guo, J.C. and Zhu, C.Q. (2009) Overexpression of F(0)F(1)-ATP synthase alpha suppresses mutant huntingtin aggregation and toxicity in vitro. *Biochem. Biophys. Res. Commun.*, **390**, 1294–1298.
25. Ruiz, M. and Deglon, N. (2012) Viral-mediated overexpression of mutant huntingtin to model HD in various species. *Neurobiol. Dis.*, **48**, 202–211.
26. de Almeida, L.P., Ross, C.A., Zala, D., Aebischer, P. and Deglon, N. (2002) Lentiviral-mediated delivery of mutant huntingtin in the striatum of rats induces a selective neuropathology modulated by polyglutamine repeat size, huntingtin expression levels, and protein length. *J Neurosci.*, **22**, 3473–3483.
27. Diguet, E., Petit, F., Escartin, C., Cambon, K., Bizat, N., Dufour, N., Hantraye, P., Deglon, N. and Brouillet, E. (2009) Normal aging modulates the neurotoxicity of mutant huntingtin. *PLoS One*, **4**, e4637.
28. Drouet, V., Perrin, V., Hassig, R., Dufour, N., Auregan, G., Alves, S., Bonvento, G., Brouillet, E., Luthi-Carter, R., Hantraye, P. *et al.* (2009) Sustained effects of nonallele-specific Huntingtin silencing. *Ann. Neurol.*, **65**, 276–285.
29. Canals, J.M., Pineda, J.R., Torres-Peraza, J.F., Bosch, M., Martin-Ibanez, R., Munoz, M.T., Mengod, G., Ernfors, P. and Alberch, J. (2004) Brain-derived neurotrophic factor regulates the onset and severity of motor dysfunction associated with enkephalinergic neuronal degeneration in Huntington's disease. *J. Neurosci.*, **24**, 7727–7739.
30. Majumder, P., Raychaudhuri, S., Chattopadhyay, B. and Bhattacharyya, N.P. (2007) Increased caspase-2, calpain activations and decreased mitochondrial complex II activity in cells expressing exogenous huntingtin exon 1 containing CAG repeat in the pathogenic range. *Cell. Mol. Neurobiol.*, **27**, 1127–1145.
31. Seo, H., Kim, W. and Isacson, O. (2008) Compensatory changes in the ubiquitin-proteasome system, brain-derived neurotrophic factor and mitochondrial complex II/III in YAC72 and R6/2 transgenic mice partially model Huntington's disease patients. *Hum. Mol. Genet.*, **17**, 3144–3153.
32. Butterworth, J., Yates, C.M. and Reynolds, G.P. (1985) Distribution of phosphate-activated glutaminase, succinic dehydrogenase, pyruvate dehydrogenase and gamma-glutamyl transpeptidase in post-mortem brain from Huntington's disease and agonal cases. *J. Neurol. Sci.*, **67**, 161–171.
33. Mann, V.M., Cooper, J.M., Javoy-Agid, F., Agid, Y., Jenner, P. and Schapira, A.H. (1990) Mitochondrial function and parental sex effect in Huntington's disease. *Lancet*, **336**, 749.
34. Brennan, W.A. Jr, Bird, E.D. and Aprille, J.R. (1985) Regional mitochondrial respiratory activity in Huntington's disease brain. *J. Neurochem.*, **44**, 1948–1950.
35. Stahl, W.L. and Swanson, P.D. (1974) Biochemical abnormalities in Huntington's chorea brains. *Neurology*, **24**, 813–819.
36. Tabrizi, S.J., Cleeter, M.W., Xuereb, J., Taanman, J.W., Cooper, J.M. and Schapira, A.H. (1999) Biochemical abnormalities and excitotoxicity in Huntington's disease brain. *Ann. Neurol.*, **45**, 25–32.
37. Turner, C., Cooper, J.M. and Schapira, A.H. (2007) Clinical correlates of mitochondrial function in Huntington's disease muscle. *Mov. Disord.*, **22**, 1715–1721.
38. Scarpulla, R.C. (2011) Metabolic control of mitochondrial biogenesis through the PGC-1 family regulatory network. *Biochim. Biophys. Acta*, **1813**, 1269–1278.
39. Scarpulla, R.C. (2011) Nucleus-encoded regulators of mitochondrial function: integration of respiratory chain expression, nutrient sensing and metabolic stress. *Biochim. Biophys. Acta*, **1819**, 1088–1097.
40. Au, H.C. and Scheffler, I.E. (1998) Promoter analysis of the human succinate dehydrogenase iron-protein gene–both nuclear respiratory factors NRF-1 and NRF-2 are required. *Eur. J. Biochem./ FEBS*, **251**, 164–174.
41. Hodges, A., Strand, A.D., Aragaki, A.K., Kuhn, A., Sengstag, T., Hughes, G., Elliston, L.A., Hartog, C., Goldstein, D.R., Thu, D. *et al.* (2006) Regional and cellular gene expression changes in human Huntington's disease brain. *Hum. Mol. Genet.*, **15**, 965–977.
42. Kuhn, A., Goldstein, D.R., Hodges, A., Strand, A.D., Sengstag, T., Kooperberg, C., Becanovic, K., Pouladi, M.A., Sathasivam, K., Cha, J.H. *et al.* (2007) Mutant huntingtin's effects on striatal gene expression in mice recapitulate changes observed in human Huntington's disease brain and do

not differ with mutant huntingtin length or wild-type huntingtin dosage. *Hum. Mol. Genet.*, **16**, 1845–1861.
43. Neupert, W. and Herrmann, J.M. (2007) Translocation of proteins into mitochondria. *Annu. Rev. Biochem.*, **76**, 723–749.
44. Klanner, C., Neupert, W. and Langer, T. (2000) The chaperonin-related protein Tcm62p ensures mitochondrial gene expression under heat stress. *FEBS Lett.*, **470**, 365–369.
45. Dibrov, E., Fu, S. and Lemire, B.D. (1998) The *Saccharomyces cerevisiae* TCM62 gene encodes a chaperone necessary for the assembly of the mitochondrial succinate dehydrogenase (complex II). *J. Biol. Chem.*, **273**, 32042–32048.
46. Ghezzi, D., Goffrini, P., Uziel, G., Horvath, R., Klopstock, T., Lochmuller, H., D'Adamo, P., Gasparini, P., Strom, T.M., Prokisch, H. *et al.* (2009) SDHAF1, encoding a LYR complex-II specific assembly factor, is mutated in SDH-defective infantile leukoencephalopathy. *Nat. Genet.*, **41**, 654–656.
47. Gonzalez-Cabo, P., Vazquez-Manrique, R.P., Garcia-Gimeno, M.A., Sanz, P. and Palau, F. (2005) Frataxin interacts functionally with mitochondrial electron transport chain proteins. *Hum. Mol. Genet.*, **14**, 2091–2098.
48. Mao, P., Ardeshiri, A., Jacks, R., Yang, S., Hurn, P.D. and Alkayed, N.J. (2007) Mitochondrial mechanism of neuroprotection by CART. *Eur. J. Neurosci.*, **26**, 624–632.
49. Cimen, H., Han, M.J., Yang, Y., Tong, Q., Koc, H. and Koc, E.C. (2010) Regulation of succinate dehydrogenase activity by SIRT3 in mammalian mitochondria. *Biochemistry*, **49**, 304–311.
50. Finley, L.W., Haas, W., Desquiret-Dumas, V., Wallace, D.C., Procaccio, V., Gygi, S.P. and Haigis, M.C. (2011) Succinate dehydrogenase is a direct target of sirtuin 3 deacetylase activity. *PloS One*, **6**, e23295.
51. Fu, J., Jin, J., Cichewicz, R.H., Hageman, S.A., Ellis, T.K., Xiang, L., Peng, Q., Jiang, M., Arbez, N., Hotaling, K. *et al.* (2012) trans-(-)-epsilon-Viniferin increases mitochondrial sirtuin 3 (SIRT3), activates AMP-activated protein kinase (AMPK), and protects cells in models of Huntington disease. *J. Biol. Chem.*, **287**, 24460–24472.
52. Wagner, G.R., Pride, P.M., Babbey, C.M. and Payne, R.M. (2012) Friedreich's ataxia reveals a mechanism for coordinate regulation of oxidative metabolism via feedback inhibition of the SIRT3 deacetylase. *Hum. Mol. Genet.*, **21**, 2688–2697.
53. Rustin, P., Munnich, A. and Rotig, A. (2002) Succinate dehydrogenase and human diseases: new insights into a well-known enzyme. *Eur. J. Hum. Genet.*, **10**, 289–291.
54. Johri, A. and Beal, M.F. (2012) Antioxidants in Huntington's disease. *Biochim. Biophys. Acta*, **1822**, 664–674.
55. Johri, A., Calingasan, N.Y., Hennessey, T.M., Sharma, A., Yang, L., Wille, E., Chandra, A. and Beal, M.F. (2012) Pharmacologic activation of mitochondrial biogenesis exerts widespread beneficial effects in a transgenic mouse model of Huntington's disease. *Hum. Mol. Genet.*, **21**, 1124–1137.
56. Xun, Z., Rivera-Sanchez, S., Ayala-Pena, S., Lim, J., Budworth, H., Skoda, E.M., Robbins, P.D., Niedernhofer, L.J., Wipf, P. and McMurray, C.T. (2012) Targeting of XJB-5–131 to mitochondria suppresses oxidative DNA damage and motor decline in a mouse model of Huntington's disease. *Cell Rep.*, **2**, 1137–1142.
57. Sims, N.R. (1990) Rapid isolation of metabolically active mitochondria from rat brain and subregions using Percoll density gradient centrifugation. *J. Neurochem.*, **55**, 698–707.
58. Damiano, M., Starkov, A.A., Petri, S., Kipiani, K., Kiaei, M., Mattiazzi, M., Flint Beal, M. and Manfredi, G. (2006) Neural mitochondrial Ca2+ capacity impairment precedes the onset of motor symptoms in G93A Cu/Zn-superoxide dismutase mutant mice. *J. Neurochem.*, **96**, 1349–1361.
59. D'Aurelio, M., Gajewski, C.D., Lenaz, G. and Manfredi, G. (2006) Respiratory chain supercomplexes set the threshold for respiration defects in human mtDNA mutant cybrids. *Hum. Mol. Genet.*, **15**, 2157–2169.
60. Schägger, H. (ed). (2003) *Membrane Protein Purification and Crystallization*. Academic Press, San Diego, CA.
61. Wittig, I., Carrozzo, R., Santorelli, F.M. and Schagger, H. (2007) Functional assays in high-resolution clear native gels to quantify mitochondrial complexes in human biopsies and cell lines. *Electrophoresis*, **28**, 3811–3820.
62. Mattiazzi, M., D'Aurelio, M., Gajewski, C.D., Martushova, K., Kiaei, M., Beal, M.F. and Manfredi, G. (2002) Mutated human SOD1 causes dysfunction of oxidative phosphorylation in mitochondria of transgenic mice. *J. Biol. Chem.*, **277**, 29626–29633.
63. Srivastava, S., Barrett, J.N. and Moraes, C.T. (2007) PGC-1alpha/beta upregulation is associated with improved oxidative phosphorylation in cells harboring nonsense mtDNA mutations. *Hum. Mol. Genet.*, **16**, 993–1005.
64. Sambrook, J. (ed). (1989) *Molecular Cloning*. Cold Spring Harbor Lab Press Plainview, New York.
65. Bell, E.L., Klimova, T.A., Eisenbart, J., Schumacker, P.T. and Chandel, N.S. (2007) Mitochondrial reactive oxygen species trigger hypoxia-inducible factor-dependent extension of the replicative life span during hypoxia. *Mol. Cell. Biol.*, **27**, 5737–5745.
66. Regulier, E., Pereira de Almeida, L., Sommer, B., Aebischer, P. and Deglon, N. (2002) Dose-dependent neuroprotective effect of ciliary neurotrophic factor delivered via tetracycline-regulated lentiviral vectors in the quinolinic acid rat model of Huntington's disease. *Hum. Gene Ther.*, **13**, 1981–1990.
67. Hottinger, A.F., Azzouz, M., Deglon, N., Aebischer, P. and Zurn, A.D. (2000) Complete and long-term rescue of lesioned adult motoneurons by lentiviral-mediated expression of glial cell line-derived neurotrophic factor in the facial nucleus. *J. Neurosci.*, **20**, 5587–5593.
68. Wong-Riley, M. (1979) Changes in the visual system of monocularly sutured or enucleated cats demonstrable with cytochrome oxidase histochemistry. *Brain Res.*, **171**, 11–28.
69. Bizat, N., Hermel, J.M., Boyer, F., Jacquard, C., Creminon, C., Ouary, S., Escartin, C., Hantraye, P., Kajewski, S. and Brouillet, E. (2003) Calpain is a major cell death effector in selective striatal degeneration induced in vivo by 3-nitropropionate: implications for Huntington's disease. *J. Neurosci.*, **23**, 5020–5030.
70. Brouillet, E., Guyot, M.C., Mittoux, V., Altairac, S., Conde, F., Palfi, S. and Hantraye, P. (1998) Partial inhibition of brain succinate dehydrogenase by 3-nitropropionic acid is sufficient to initiate striatal degeneration in rat. *J. Neurochem.*, **70**, 794–805.
71. Ackrell, B.A., Kearney, E.B. and Singer, T.P. (1978) Mammalian succinate dehydrogenase. *Methods Enzymol.*, **53**, 466–483.
72. Dubois, A., Dauguet, J., Herard, A.S., Besret, L., Duchesnay, E., Frouin, V., Hantraye, P., Bonvento, G. and Delzescaux, T. (2007) Automated three-dimensional analysis of histological and autoradiographic rat brain sections: application to an activation study. *J. Cereb. Blood Flow Metab.*, **27**, 1742–1755.